High-performance laterally-arranged multiple-bandgap solar cells using spatially composition-graded $Cd_xPb_{1-x}S$ nanowires on a single substrate: a design study

D. A. Caselli and C. Z. Ning*

School of Electrical, Computer, and Energy Engineering, Arizona State University, Tempe, Arizona 85287, USA
**cning@asu.edu*

Abstract: In this paper, laterally arranged multiple bandgap (LAMB) solar cells based on $Cd_xPb_{1-x}S$ alloy nanowires of varying composition on a single substrate are designed to be used together with a dispersive concentrator. Simulation results for a design with six subcells in series connection are presented. The design is based on a unique materials capability achieved in our recent research. An efficiency of 34.9% was obtained for operation without solar concentration, which increased to 40.5%, 41.7%, and 42.7% for concentration ratios of 25, 100, and 240 respectively. The device was also simulated with decreased carrier mobilities to model the possible reduction in absorber conductivity, depending on the nanowire geometry and configuration. For a concentration ratio of unity, decreasing the mobilities to 25% of their original values caused less than a 2.5% absolute drop in efficiency. The LAMB design offers the advantages of an integrated cell platform and the potential for low-cost, high efficiency photovoltaic systems.

OCIS codes: (350.6050) Solar energy; (040.5350) Photovoltaic.

References and links

1. M. A. Green, *Third Generation Photovoltaics: Advanced Solar Energy Conversion* (Springer-Verlag, 2006).
2. M. A. Green, K. Emery, Y. Hishikawa, and W. Warta, "Solar cell efficiency tables (version 35)," Prog. Photovolt. Res. Appl. **18**(2), 144–150 (2010).
3. N. A. Gokcen and J. J. Loferski, "Efficiency of tandem solar cell systems as a function of temperature and solar energy concentration ratio," Sol. Energy Mater. **1**(3-4), 271–286 (1979).
4. W. H. Bloss, M. Griesinger, and E. R. Reinhardt, "Dispersive concentrating systems based on transmission phase holograms for solar applications," Appl. Opt. **21**(20), 3739–3742 (1982).
5. A. Barnett, D. Kirkpatrick, C. Honsberg, D. Moore, M. Wanlass, K. Emergy, R. Schwartz, D. Carlson, S. Bowden, D. Aiken, A. Gray, S. Kurtz, L. Kazmerski, T. Moriarty, M. Steiner, J. Gray, T. Davenport, R. Buelow, L. Takacs, and N. Shatz, "Milestones toward 50% efficiency solar cell modules," Presented at the *22nd European Photovoltaic Solar Energy Conference* (Institute of Electrical and Electronics Engineers, Milan, Italy, 2007).
6. A. L. Pan, W. Zhou, E. S. P. Leong, R. B. Liu, A. H. Chin, B. Zou, and C. Z. Ning, "Continuous alloy-composition spatial grading and superbroad wavelength-tunable nanowire lasers on a single chip," Nano Lett. **9**(2), 784–788 (2009).
7. T. Kuykendall, P. Ulrich, S. Aloni, and P. Yang, "Complete composition tunability of InGaN nanowires using a combinatorial approach," Nat. Mater. **6**(12), 951–956 (2007).
8. A. L. Pan, R. B. Liu, M. Sun, and C. Z. Ning, "Spatial composition grading of quaternary ZnCdSSe alloy nanowires with tunable light emission between 350 and 710 nm on a single substrate," ACS Nano **4**(2), 671–680 (2010).
9. C. Z. Ning, A. L. Pan, and R. B. Liu, "Spatially composition-graded alloy semiconductor nanowires and wavelength specific lateral-multijunction full-spectrum solar cells," in *Proceedings of the 34th IEEE Photovoltaic Specialists Conference* (Institute of Electrical and Electronics Engineers, Philadelphia, Pennsylvania, 2009), pp. 001492–001495.
10. J. E. Ludman, J. Riccobono, I. V. Semenova, N. O. Reinhand, W. Tai, X. Li, G. Syphers, E. Rallis, G. Sliker, and J. Martín, "The optimization of a holographic system for solar power generation," Sol. Energy **60**(1), 1–9 (1997).
11. J. R. Riccobono, H. J. Caulfield, and J. E. Ludman, *Holography for the New Millennium* (Springer-Verlag, 2002).
12. ATLAS, version 5.15.34.C, Silvaco Data Systems, Inc.: 2009.

#142384 - $15.00 USD Received 9 Feb 2011; revised 14 May 2011; accepted 14 May 2011; published 17 May 2011

13. H. Rahnamai and J. N. Zemel, "PbS – Si heterojunction II: electrical properties," Thin Solid Films **74**(1), 17–22 (1980).
14. Z. Liu, J. H. Kim, G. E. Fernandes, and J. Xu, "Room temperature photocurrent response of PbS/InP heterojunction," Appl. Phys. Lett. **95**(23), 231113 (2009).
15. *ATLAS User's Manual: Device Simulation Software* (SILVACO International, 2007).
16. T. L. Chu and S. S. Chu, "Thin film II-VI photovoltaics," Solid-State Electron. **38**(3), 533–549 (1995).
17. E. Kymakis and G. A. Amaratunga, "Single-wall carbon nanotube/conjugated polymer photovoltaic devices," Appl. Phys. Lett. **80**(1), 112–114 (2002).
18. U. V. Desnica, "Doping limits in II-VI compounds – challenges, problems and solutions," Prog. Cryst. Growth Charact. Mater. **36**(4), 291–357 (1998).
19. Y. Imai, A. Watanabe, and I. Shimono, "Comparison of electronic structures of doped ZnS and ZnO calculated by a first-principle pseudopotential method," J. Mater. Sci. Mater. Electron. **14**(3), 149–156 (2003).
20. H. Ohta, M. Orita, M. Hirano, H. Tanji, H. Kawazoe, and H. Hosono, "Highly electrically conductive indium-tin-oxide thin films epitaxially grown on yttria-stabilized zirconia (100) by pulsed-laser deposition," Appl. Phys. Lett. **76**(19), 2740–2742 (2000).
21. A. Mondal, B. E. McCandless, and R. W. Birkmire, "Electrochemical deposition of thin ZnTe films as a contact for CdTe solar cells," Sol. Energy Mater. Sol. Cells **26**(3), 181–187 (1992).
22. D. J. Friedman and J. M. Olson, "Analysis of Ge Junctions for GaInP/GaAs/Ge Three-junction Solar Cells," Prog. Photovolt. Res. Appl. **9**(3), 179–189 (2001).
23. K. Emery and D. Meyers, "Solar Spectral Irradiance: Air Mass 1.5" (National Renewable Energy Laboratory, 2009). *http://rredc.nrel.gov/solar/spectra/am1.5/ASTMG173/ASTMG173.html*.
24. M. D. Kelzenberg, S. W. Boettcher, J. A. Petykiewicz, D. B. Turner-Evans, M. C. Putnam, E. L. Warren, J. M. Spurgeon, R. M. Briggs, N. S. Lewis, and H. A. Atwater, "Enhanced absorption and carrier collection in Si wire arrays for photovoltaic applications," Nat. Mater. **9**(3), 239–244 (2010).
25. N. Lagos, M. M. Sigalas, and D. Niarchos, "The optical absorption of nanowire arrays," Photon. Nanostruct. Fundam. Appl. **9**(2), 163–167 (2011), doi:10.1016/j.photonics.2010.09.005.
26. M. M. Sigalas, Institute of Materials Science, N.C.S.R "Demokritos" Agia Paraskevi, 15310 Athens, Greece (personal communication, 2010).
27. R. R. King, D. C. Law, K. M. Edmondson, C. M. Fetzer, G. S. Kinsey, H. Yoon, R. A. Sherif, and N. H. Karam, "40% efficient metamorphic GaInP / GaInAs / Ge multijunction solar cells," Appl. Phys. Lett. **90**(18), 183516 (2007).
28. Z. Fan, J. C. Ho, Z. A. Jacobson, R. Yerushalmi, R. L. Alley, H. Razavi, and A. Javey, "Wafer-scale assembly of highly ordered semiconductor nanowire arrays by contact printing," Nano Lett. **8**(1), 20–25 (2008).
29. P. Yang and F. Kim, "Langmuir-Blodgett assembly of one-dimensional nanostructures," ChemPhysChem **3**(6), 503–506 (2002).
30. Z. Fan, H. Razavi, J. W. Do, A. Moriwaki, O. Ergen, Y. L. Chueh, P. W. Leu, J. C. Ho, T. Takahashi, L. A. Reichertz, S. Neale, K. Yu, M. Wu, J. W. Ager, and A. Javey, "Three-dimensional nanopillar-array photovoltaics on low-cost and flexible substrates," Nat. Mater. **8**(8), 648–653 (2009).

1. Introduction

High system cost remains the most significant barrier to wide scale adoption of photovoltaic energy. Thin-film solar cells aim to reduce the cost of solar modules by decreasing material consumption, and they have made significant progress in this respect. However, it is argued [1] that the cost of mature thin film photovoltaic modules will, like silicon cells, be dominated by their materials costs, and therefore modules based on high efficiency cells are likely to replace them. Much of the research on high-efficiency terrestrial photovoltaics currently focuses on using expensive tandem cells established for space applications in concentrator systems where their high efficiencies enable reductions in total system costs. The industry standard in this area is Spectrolab's GaInP/GaInAs/Ge triple-junction tandem cell, which boasts an efficiency of over 41% under 364 times concentrated sunlight [2]. Significant performance improvements with triple-junction solar cells are probably not practical, as Gokcen and Loferski estimate that a triple-junction cell can obtain about 45% efficiency at concentration levels of 500 to 1000 suns, so the natural strategy is simply to add more junctions [3]. However, the practical number of junctions in a vertically stacked tandem cell is limited by the lattice-matching constraint, the availability of bandgaps at the desired values, and the ability to construct proper tunneling junctions. All these factors make significantly increasing the number of junctions exceedingly difficult.

Absorption of different solar spectral components by different bandgaps can also be accomplished in parallel by using LAMB solar cells, which are not bound by the lattice-matching requirement. Such LAMB cells require a dispersive optics layer to spectrally split the sunlight onto different bandgap regions such that each spectral band is absorbed by the

#142384 - $15.00 USD Received 9 Feb 2011; revised 14 May 2011; accepted 14 May 2011; published 17 May 2011

optimized bandgap. The concept of dispersive concentration photovoltaics (DCPV), illustrated schematically in Fig. 1, has been studied since the early 1980s [4]. One of the most recent attempts related to the current approach is the Very High Efficiency Solar Cell (VHESC) program, in which the researchers combined existing solar cell designs with optics for spectral splitting [5]. They estimated that the structure could achieve 50% overall system efficiency using a low concentration ratio of about 20 [5]. However, all DCPV approaches [4,5] so far have used discrete solar cells on different material platforms, arranged spatially to absorb different spectral components. Such approaches, while important in demonstrating the feasibility of DCPV, are too bulky, complex, and expensive to be practical over the long run. A preferable approach would be to fabricate all subcells simultaneously on a single substrate and integrate them with dispersive optics. Such a capability is provided by recent progress in the growth of alloy nanowires by our group.

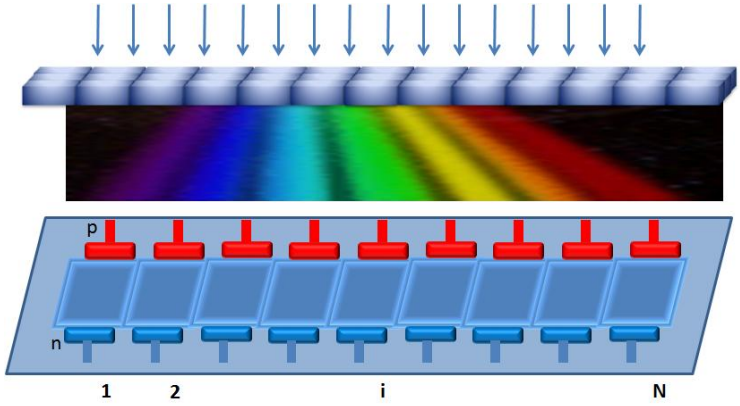

Fig. 1. Conceptual schematic of a LAMB solar cell with a spectral splitting concentration optics layer.

Using a "dual gradient" growth method, which combines a temperature gradient [6] with spatial reagent profiling [7] across the surface of a substrate, our group was recently able to grow semiconductor alloy nanowires with the alloy composition continuously varying over a wide range on a single substrate [6,8]. The corresponding band edge emission wavelength spans the entire visible spectrum across the substrate length [6,8]. Such material capability would provide a natural choice as wavelength specific absorption cells for a LAMB design, allowing the absorbing materials in all subcells of a LAMB system to be grown in a single CVD growth [6,8,9]. The pre-patterning of the substrate and the selective deposition of catalyst materials assure that the different subcells are laterally separated. Spatially composition graded CdS_xSe_{1-x} and $Zn_xCd_{1-x}S_ySe_{1-y}$ nanowires have already been grown successfully in this way over their complete composition ranges [6,8]. Work is presently underway to achieve similar results with $Cd_xPb_{1-x}S$, which can cover essentially the entire spectral range of interest to photovoltaics.

Spectral splitting could be accomplished using a holographic dispersive concentrator (HDC) which is light-weight, inexpensive, and has high optical efficiency over a broad spectral range [4,10,11]. Holographic elements are particularly advantageous because spectral splitting and solar concentration can be performed simultaneously by the same optical element, facilitating higher efficiencies, reducing system weight and complexity, and ultimately enabling lower costs [11]. In addition, the compact form-factors of HDCs match perfectly with the monolithic lateral subcells, so that eventually the two components can be integrated.

This paper will describe the design of a LAMB solar cell based on spatially composition graded $Cd_xPb_{1-x}S$ nanowires to be used in conjunction with a compact dispersive concentrating optical layer such as an HDC. Simulation results obtained using Silvaco

#142384 - $15.00 USD Received 9 Feb 2011; revised 14 May 2011; accepted 14 May 2011; published 17 May 2011

ATLAS [12] software will be presented and discussed. The design of an HDC is discussed elsewhere by other researchers [4,10].

2. Design

The range of bandgaps available using $Cd_xPb_{1-x}S$ stretches approximately from 0.4 eV (PbS) [13–15] to 2.4 eV (CdS) [15,16]. To design the subcells for optimal series connections, it is necessary to choose the bandgaps such that equal numbers of photons impinge on each, assuming the number of electron-hole pairs extracted per incident photon is approximately the same for all subcells. Six subcells were chosen for the simulation, with a minimum bandgap of 0.7 eV, which set the composition of all subcells as shown in Table 1. The layout of the entire structure is shown in Fig. 2.

The structure of each subcell consists of a transparent top contact, a window layer, intrinsic $Cd_xPb_{1-x}S$ nanowires, a back-surface field (BSF) layer, and a rear electrode. The heavily doped window and BSF layers create electric fields in the intrinsic nanowires which accelerate electrons and holes towards the negative and positive electrodes respectively. Ideally, they should also readily accept charge carriers of one type from the nanowires while blocking carriers of the opposite type. This prevents electrons generated near the p-contact or holes generated near the n-contact from diffusing toward the wrong electrode, thereby decreasing the output of the cell. Both ends of the nanowires could ideally be embedded inside the doped layers to improve the contacts and facilitate carrier collection.

Table 1. $Cd_xPb_{1-x}S$ Composition and Material Data by Subcell

Subcell	Composition	Bandgap (eV)	Electron Affinity (eV)
1	$Cd_{0.89}Pb_{0.11}S$	2.17	4.36
2	$Cd_{0.64}Pb_{0.36}S$	1.67	4.07
3	$Cd_{0.52}Pb_{0.48}S$	1.43	3.93
4	$Cd_{0.39}Pb_{0.61}S$	1.17	3.77
5	$Cd_{0.28}Pb_{0.72}S$	0.95	3.64
6	$Cd_{0.16}Pb_{0.84}S$	0.70	3.50

The broad range of bandgaps and electron affinities spanned by these nanowires poses a design challenge for effective extraction of photogenerated carriers. The window and BSF layers must be heavily doped and have minimal band offsets with the band edges of the carriers they are designed to extract. This poses a greater challenge to the p-contacts because the positions of the valence band edges vary through a larger range than the conduction band edges. This, in addition to the fact that nearly all common transparent conductors are n-type, makes it convenient to choose the top contact to be n-type. The electron affinities of $Cd_xPb_{1-x}S$ for many subcells are relatively small; therefore a transparent n-type conductor with a low work function or a highly doped semiconductor with a low electron affinity is required for the window layer. The most common transparent conductor, indium tin oxide (ITO), has a work function of approximately 4.7 eV, which is too large to effectively extract electrons from $Cd_xPb_{1-x}S$ [17]. The bandgap of ZnS, at 3.66 eV, is large enough for the material to be transparent for all wavelengths of interest, and it has an appropriately small electron affinity at 3.9 eV [16]. ZnS can be n-doped above 10^{19} cm^{-3} [18], but unfortunately its conductivity is still an order of magnitude below that of ITO [19,20]. Therefore, the most appropriate top contact structure consists of a thin film of heavily-doped ZnS as a window layer, deposited on an ITO-coated glass substrate, which serves as the transparent n-contact.

For the BSF layers and p-contacts, it is not possible to use the same materials across all subcells due to the large range through which the positions of the valence band edges vary. Therefore, p-ZnTe is used for the BSF layers of the three largest bandgap subcells and p-Ge is used for the three smallest bandgap subcells (Fig. 2). The energy band lineups are shown in Fig. 3.

#142384 - $15.00 USD Received 9 Feb 2011; revised 14 May 2011; accepted 14 May 2011; published 17 May 2011

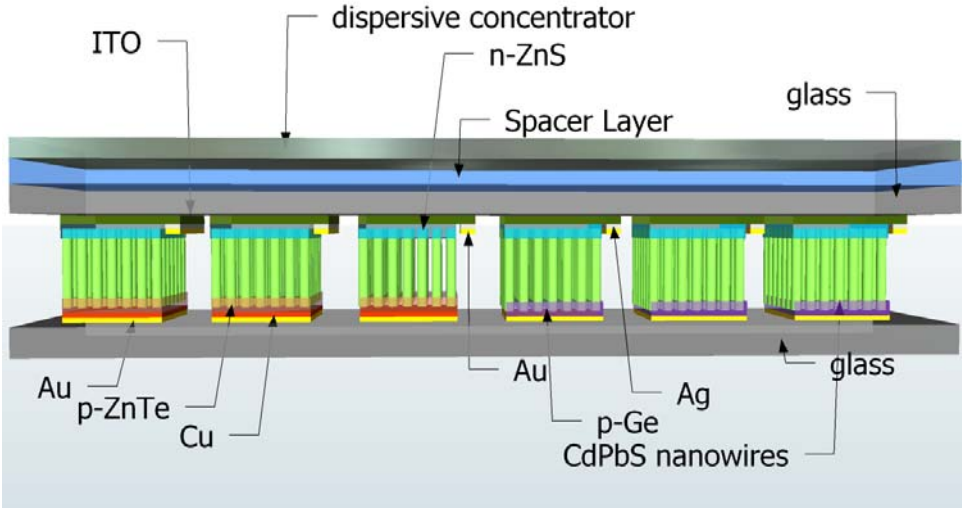

Fig. 2. LAMB solar cell structure with n-ZnS/ITO n-contacts and p-ZnTe or p-Ge p-contacts to undoped CdxPb1-xS nanowires.

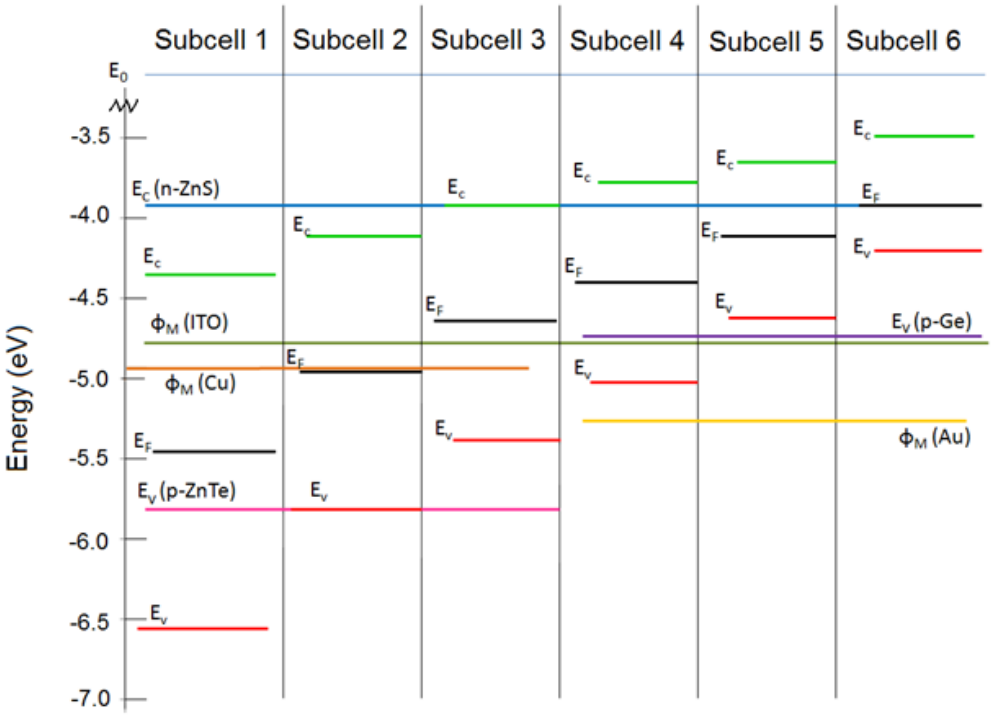

Fig. 3. Energy band lineup of CdxPb1-xS nanowires with the contact materials across all subcells according to Anderson's Model. Note that the Fermi levels of the CdxPb1-xS nanowires assume intrinsic material.

Lastly, materials must be selected for the final metal-semiconductor contacts. Cu is the most appropriate choice of metal to contact p-ZnTe because it acts as an acceptor in this material, and therefore diffusion of the Cu metallization into the ZnTe helps to create a highly doped layer near the surface that facilitates tunneling [21]. Au is used to form ohmic contacts

#142384 - $15.00 USD Received 9 Feb 2011; revised 14 May 2011; accepted 14 May 2011; published 17 May 2011

to p-Ge in GaInP/GaInAs/Ge tandem cells [22], making it a natural choice to contact p-Ge here as well.

3. Simulations

Computer simulations of the solar cell described above were conducted using Silvaco ATLAS device simulation software [12] with the ASTM G173 standard air mass 1.5 direct spectrum as the simulated illumination source [23]. Due to practical considerations, a number of simplifying assumptions were made:

1) In all cases, ideal ohmic contacts to the window and BSF layers were assumed. These layers were all simulated using dopant concentrations of 10^{19} cm^{-3}.

2) Spectral splitting was assumed to occur with no optical loss, and reflection at the top interfaces of the subcells was ignored, equivalent to assuming an ideal anti-reflective coating.

3) All subcells were assumed to have equal surface areas.

4) For the sake of simplicity, the $Cd_xPb_{1-x}S$ absorbing material was assumed to be a thin film 2 μm thick for all subcells in our simulation. Thus one might argue that a spatial filling factor smaller than unity should be applied if it is to properly simulate a nanowire array due to the existence of voids. However, studies have shown that nanowire arrays have significantly enhanced light absorption properties compared to continuous thin films for certain spatial filling factors [24,25]. For the case of Si nanowires, it has been shown that a vertical nanowire array with an areal filling ratio of 0.2 or 0.44 has superior absorption characteristics to a planar Si surface [25,26]. The final balance of the two effects would modify the simulation results that follow, depending upon the spatial filling factor of the nanowire array. In addition, the effective conductivity of the nanowire layers may be somewhat smaller than that of a continuous film due to surface scattering and possibly, in the case of randomly oriented nanowires, small contact areas between wires. This effect has been studied by performing simulations with various levels of reduced carrier mobilities.

5) Material bandgaps, electron affinities, wavelength dependent real and imaginary parts of the refractive indices, effective densities of states, and carrier mobilities for $Cd_xPb_{1-x}S$ were calculated by simple linear interpolation based on the composition fraction.

6) The composition of the $Cd_xPb_{1-x}S$ nanowires was assumed to be fixed in any given subcell.

7) Only Shockley-Read-Hall recombination was considered, with fixed carrier lifetimes of 10 ns for all materials.

The simulations were performed for solar concentration ratios of one, 25, 100, and 240, defined as the area of the solar collector (HDC) divided by the area of the solar cell. Note that spectral splitting entails that all sunlight within a given spectral range incident on the HDC is focused on a single subcell. Given that there are six subcells of equal areas, this means that the portion of the spectrum assigned to any individual subcell is effectively already concentrated by a factor of six even for a solar concentration ratio of one. The efficiencies under various levels of solar concentration are shown in Table 2.

The graphs in Fig. 4 show the current-voltage characteristics for all the subcells individually at the various concentration ratios. Several features of these curves bear examination. The current-voltage characteristic of the first (largest bandgap) subcell flattens as the current density approaches zero, an effect known as “roll-over”. This is due to the large valence band offset at the interface with the BSF layer; the valence band of p-ZnTe is significantly above that of $Cd_{0.89}Pb_{0.11}S$. A significant improvement in the performance of this

#142384 - $15.00 USD Received 9 Feb 2011; revised 14 May 2011; accepted 14 May 2011; published 17 May 2011

solar cell could be achieved if a suitable alternative to p-ZnTe were found for the first subcell with its valence band closer to that of $Cd_{0.89}Pb_{0.11}S$. Also note that the sixth (smallest bandgap) subcell is current limiting. This indicates lower external quantum efficiency than in the other subcells due to less efficient charge separation. The problem in this case is that the valence band of $Cd_{0.16}Pb_{0.84}S$ is significantly higher than that of Ge, as shown in Fig. 3. This presents a barrier to hole extraction and tends to decrease the magnitude of the electric field in the nanowires, hindering charge separation. This can be seen in Fig. 5, which shows the band diagrams for all subcells operating at the maximum power point. Note that the bands in subcell 6 are relatively flat, indicating that it is operating reasonably close to the short-circuit point, as expected for the current-limiting subcell at the maximum power point of the overall LAMB solar cell.

The efficiencies shown in Table 2 are competitive with existing tandem cells [27]. A metamorphic GaInP/GaInAs/Ge tandem solar cell from Spectrolab achieved 40.7% efficiency at 240 suns, about 2% (absolute) less than that of the simulated LAMB solar cell [27]. Additionally, due to the many layers that must be deposited one-by-one to make these tandem cells, the fabrication of a lateral multijunction $Cd_xPb_{1-x}S$ cell could potentially be much simpler and therefore less expensive. Potential improvements with respect to the BSF layers and charge separation could even increase the efficiency further. One such improvement would be to replace p-Ge with p-Si in the fourth subcell. This would increase the efficiencies shown in Table 2 to 35.5%, 41.3%, 42.6%, and 43.7% for concentration ratios of one, 25, 100, and 240 respectively, which represents a gain of 1% (absolute) efficiency for the highest concentration ratio at the expense of greater complexity. Given materials with ideal band lineups to $Cd_xPb_{1-x}S$, efficiencies as high as 40.7%, 48.2%, 51.2%, and 53.1% were achieved in simulations for concentration ratios of one, 25, 100, and 240, respectively.

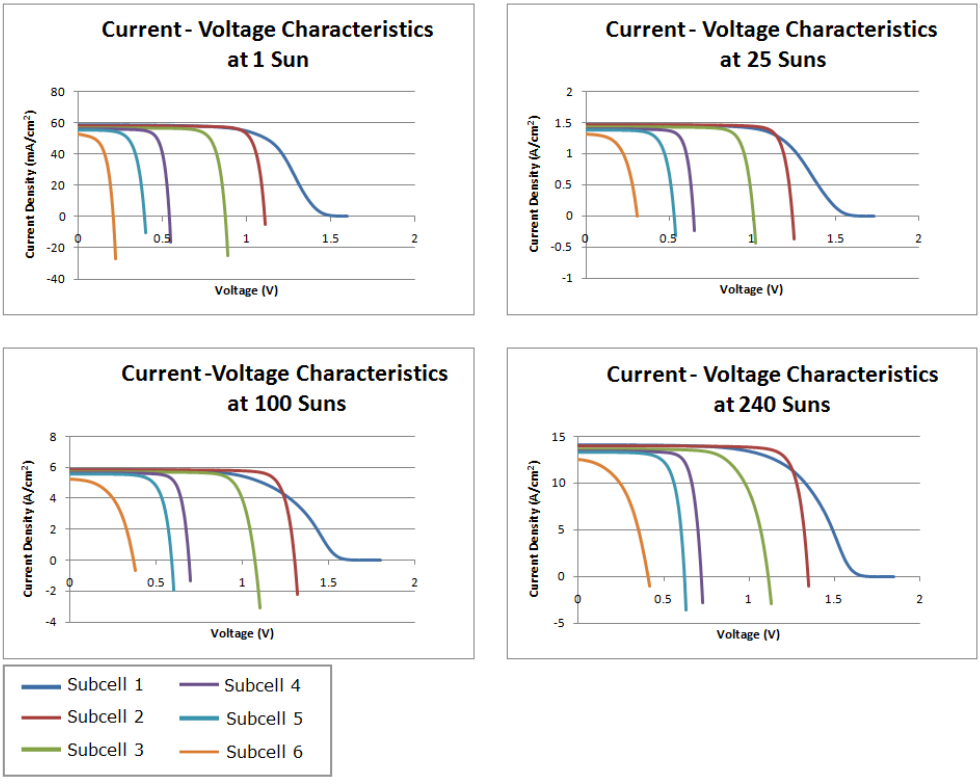

Fig. 4. Current-voltage characteristics of all subcells at varying levels of solar concentration.

#142384 - $15.00 USD Received 9 Feb 2011; revised 14 May 2011; accepted 14 May 2011; published 17 May 2011

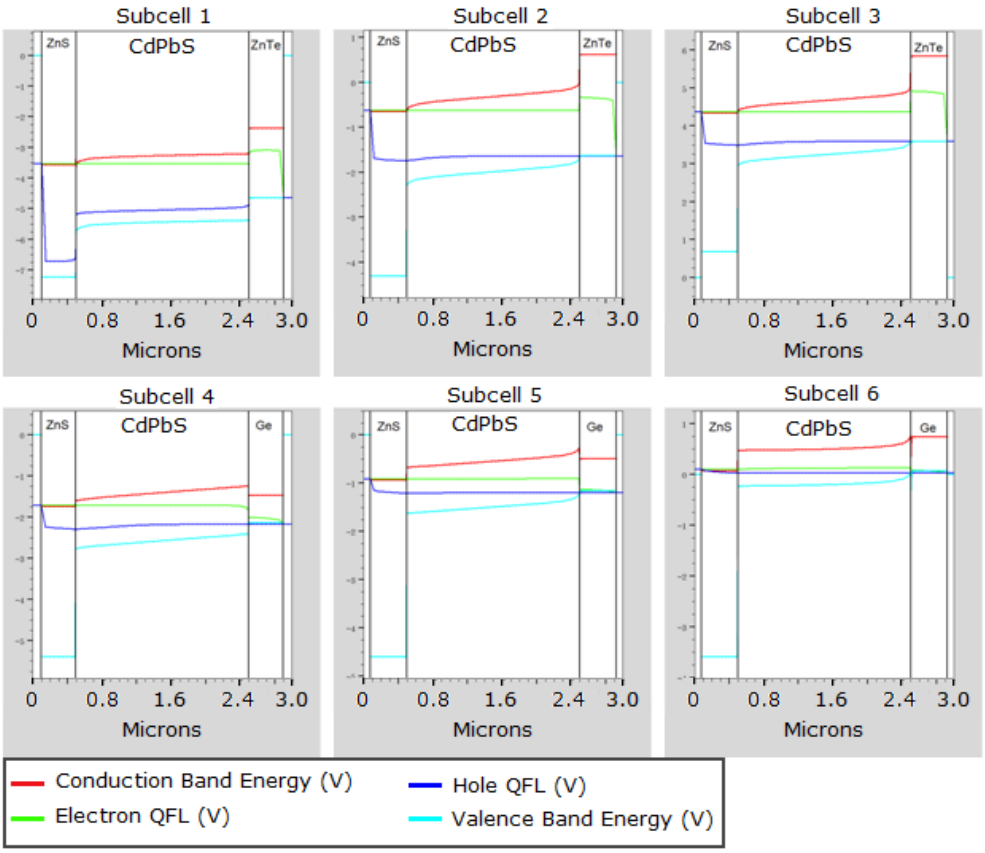

Fig. 5. Energy band diagrams at the maximum power point under one sun illumination. However, as previously mentioned, the conductivity in the $Cd_xPb_{1-x}S$ nanowire layer may be lower than in a thin film, especially if the wires are randomly oriented and mostly parallel to device layers. Therefore, these simulations were repeated with carrier mobilities reduced to 50% and 25% of their original values. The efficiencies with respect to mobility and solar concentration are shown in Table 2. The LAMB solar cell maintains sufficient performance even with the mobilities reduced by 50% to make it an attractive prospect for generating electricity.

Table 2. Efficiencies at Various Levels of Solar Concentration and with Carrier Mobilities at 100%, 50%, and 25% of their Original Values

Mobilities	Concentration	η	FF	V_{oc} (V)	J_{sc} (mA/cm^2)
100%	1	34.9%	78.3%	4.593	8.739
100%	25	40.5%	79.6%	5.236	218.6
100%	100	41.7%	77.3%	5.556	874.1
100%	240	42.7%	74.7%	5.899	2091
50%	1	33.9%	77.4%	4.549	8.652
50%	25	39.3%	76.3%	5.343	216.6
50%	100	38.9%	72.6%	5.571	866.0
50%	240	38.4%	68.4%	5.901	2058
25%	1	32.5%	77.0%	4.473	8.487
25%	25	37.5%	74.9%	5.287	212.9
25%	100	35.4%	66.1%	5.663	851.0
25%	240	32.1%	66.9%	5.597	1856

4. Fabrication

There are a number of possible approaches to fabricating LAMB cells using either randomly oriented or vertical nanowire arrays. Randomly oriented nanowires may be transferred to

#142384 - $15.00 USD Received 9 Feb 2011; revised 14 May 2011; accepted 14 May 2011; published 17 May 2011

another substrate by contact printing [28] or the Langmuir-Blodgett technique [29] to order them sufficiently before deposition of the contact materials. Spin-on-glass, Si_3N_4 or SiO_2 deposited by CVD can be used to isolate the p and n-type contacts. The insulating material can be etched to expose the nanowires prior to contact deposition to ensure good electrical contact. Alternatively, vertical nanowire arrays can be obtained using growth templates such as those made from anodized aluminum oxide (AAO). The AAO would serve essentially the same purpose as the dielectric material for the randomly oriented wires, isolating the p and n-type contact materials from each other and providing a planar surface for film deposition. The AAO can be etched using NaOH to expose the nanowires before depositing the contact materials to obtain better electrical contact [30].

The exact details of growing $Cd_xPb_{1-x}S$ nanowires with or without templates and controlling the spatial composition distribution are still part of ongoing research. As in any engineered system, some amount of manufacturing error is inevitable, so it is likely that there may be mismatches between the energies of photons incident on a subcell and those for which it was designed, however this is not catastrophic. Some such losses may occur, but a well-optimized growth and fabrication process should minimize these.

5. Conclusion

We have proposed an integrated platform for the laterally arranged multiple bandgap solar cells to be integrated with low-cost, compact dispersive concentration optics for DCPV applications. A design study of LAMB solar cells using composition graded alloy nanowires has been conducted. This design was simulated using Silvaco ATLAS device simulation software [12], and the results demonstrate that spatially composition graded $Cd_xPb_{1-x}S$ nanowires have the potential to deliver efficiencies competitive with the other high efficiency solar cells on the market today. Moreover, the ability to vary the bandgaps of these nanowires over a broad spectral range on a single substrate using the dual gradient growth method [6], [8] offers the possibility of significantly reducing manufacturing costs by simplifying the fabrication process. The proposed fabrication including deposition of doped contact layers and the growth of alloy nanowires can all be accomplished using low cost CVD methods. Other material systems besides $Cd_xPb_{1-x}S$ can also be used for LAMB cells, including $In_xGa_{1-x}N$, which other researchers recently used to grow spatially composition graded alloy nanowires [7]. Like $Cd_xPb_{1-x}S$, $In_xGa_{1-x}N$ can achieve bandgaps spanning the entire range of wavelengths of interest for photovoltaics, making it another excellent candidate for use in LAMB solar cells. The potential for high performance and cost effective fabrication of LAMB solar cells based on this technology makes them an attractive prospect for decreasing the cost per watt of photovoltaic energy. Several other advantages of this approach are also worthy of mention, including the ability to easily and significantly increase the number of junctions and the flexibility to choose different connection schemes for the subcells (unlike tandem cells, which are restricted to series connections). However, many challenges remain to be faced in research and development before this design becomes practical.

Acknowledgments

Derek Caselli would like to thank the Science Foundation of Arizona (SFAz) for their generous financial support in the form of a graduate research fellowship, Kang Ding and Debin Li for valuable technical discussions, Patricia Nichols for proofreading this article, and Arizona State University for providing Silvaco simulation software. Initial funding from the SFAz was greatly appreciated. Financial support from the Army Research Office for the growth of composition graded alloy nanowires led to the ideas investigated here.

#142384 - $15.00 USD Received 9 Feb 2011; revised 14 May 2011; accepted 14 May 2011; published 17 May 2011